Biointerface Research in Applied Chemistry
Platinum Open Access Journal (ISSN: 2069-5837)

Article
Volume 11, Issue 2, 2021, 8875 - 8883
https://doi.org/10.33263/BRIAC112.88758883

Biosynthesized Ag Nanoparticles: a Promising Pathway for Bandgap Tailoring

Jicksy Joy [1], Mithun Sanadi Gurumurthy [1], Riya Thomas [1], Manoj Balachandran [4,*]

[1] Department of Physics & Electronics, CHRIST (Deemed to be University), Bangalore, India; jicksyjoy13@gmail.com (J.J.); mithun.g@phy.christuniversity.in (M.S.G.); riyapooppillil@gmail.com (R.T.); manoj.b@christuniversity.in (M.B.);
* Correspondence: manoj.b@christuniversity.in;

Scopus Author ID 36626120900
Received: 7.07.2020; Revised: 14.08.2020; Accepted: 15.08.2020; Published: 21.08.2020

Abstract: The unrivaled features and prospective applications promote graphene as a potent contender for next-generation nanodevices. But the realization of a tunable bandgap structure for zero-bandgap graphene at all times persists as a dilemma. In this work, a green approach is adopted for the bandgap modulation of graphene oxide (GO). The biosynthesized silver nanoparticles (AgNPs) were introduced into the graphene matrix, and hence the bandgap was tailored for the formation of a semiconductor composite. The bare GO that has got a bandgap of 3.41 eV was tuned to 2.33 eV on the addition of AgNPs. The preparation of AgNPs using fruit extract of *cyanococcus* make the process greener, safer, and cost-effective. This paper intends to open a new venture towards the environment safe synthesis of semiconductor nanocomposite necessitate for optoelectronic and photovoltaic technologies.

Keywords: biosynthesis; silver nanoparticles; nanocomposite; bandgap tailoring.

1. Introduction

The intriguing characteristics of graphene have exponentially accelerated the uptake of research among the scientific community [1,2]. The high electron mobility, ultrafast optical response, and high stability of graphene encouraged its utilization towards the fabrication of advanced electronics [3-5]. However, the necessity of a tunable bandgap structure is the practical challenge that hinders the extended application of graphene systems. Although there are several ways for tailoring bandgap, oxygen functionalization is a solitary approach for deriving linear correlation between the bandgap of the material with the Carbon/Oxygen (C/O) ratio [6]. Graphene oxide (GO), the monolayer of graphene comprises oxygen-based functional groups such as hydroxyl (-OH), carbonyl (C-O), alkoxy (C-O-C), and carboxyl (-COOH) groups. There are many reports on bandgap opening with the insertion of oxygen, and hence GO can grant a tunable band structure [7,8]. However, the controlled reduction of oxygen moieties over the carbon framework can facilitate the modification of the surface, physical, chemical, optical and electronic properties. The reduction level of oxygen is majorly dependent on factors such as temperature, reducing agents, intercalates in GO, and so on [9]. The reduction of GO at elevated temperature requires not only ambient conditions but also induce numerous defects in the graphene sheets. This leads to the formation of additional carbonyl at intermediate temperature due to the reaction of water molecules at the defect sites [10]. The wet chemistry protocol is often dealt with the use of aggressive and chemical reducing agents.

Therefore, thermal or chemical-free approaches are more desirable for an environmentally innocuous technique for bandgap modulation.

Interfacing of metal nanoparticles with GO prevents the agglomeration of graphene sheets and also formulate an advanced composite material. Due to the synergistic effect between graphene and metal nanostructures, the distinctive capabilities of the composite are much enhanced than that of individual components separately [11,12]. Among noble metal nanoparticles, silver nanoparticles (AgNPs) gained increased attention owing to its exceptional photonic and electronic features. AgNPs showcase the phenomenon known as surface plasmon resonance in the visible spectrum due to its resonant vibration on interaction with incident photons [13]. This plasmon silver can also assist in the increased electron transfer, which is complimentary for graphene that can either store or transport electrons [14,15]. Henceforth, the Graphene-silver hybrid system meets the criterion for a semiconductor composite intended for applications such as solar cells, photocatalyst, sensors, and so on.

The intercalation of silver nanoparticles in the graphene matrix was achieved through various synthesis techniques. Das and co-workers adopted the in-situ chemical reduction technique utilizing $NaBH_4$ for the preparation of GO-Ag nanocomposite [16]. The photo-assisted reduction was employed to prepare reduced graphene oxide-Ag composite in which phosphotungstate ($PW_{12}O_{40}^{4-}$) was used as a photocatalyst under UV light irradiation [17]. Heena *et al.* confirmed the deposition of AgNPs over the graphene surface under microwave irradiation using hydrazine hydrate as the dispersing and reducing agent [18]. Ultra sonication technique was performed on the solution of graphene oxide and silver nanoparticles prepared in methanol to synthesize GO-Ag nanocomposite [19]. However, the toxicity of reducing agents, generation of high heat, and requirement of sophisticated techniques in the conventional methods instigated ecologically pristine approaches for the preparation of the GO-Ag hybrid system.

Green nanoparticle synthesis consists of environmentally benign reducing or capping agents that make the process safer and cost-effective. Plant-mediated nanoparticles do not require an additional surfactant or template for the stabilization. The fruit *cyanococcus* (Blueberry) is rich in biomolecules, antioxidants, and anthocyanin compounds, which can help in the reduction and stabilization of nanoparticles. In this work, blueberry extract is used for the synthesis of silver nanoparticles and the formulation of GO-Ag nanocomposite.

Understanding the immense possibility of graphene-metal nanostructures towards organic nanoelectronics, we consider it is worthwhile to investigate the bandgap modulation of graphene derivatives using biosynthesized silver nanoparticles. In the light of recent literature, the studies on the bandgap tuning and optical properties of GO-Ag composite synthesized via greener and sustainable processes are hardly found. We hereby report the optical bandgap tuning of graphene nanocomposite by the addition of AgNPs. The interplay play between the graphene structure and metal nanoparticle towards the preparation of semiconducting nanocomposite is systematically investigated.

2. Materials and Methods

2.1. Materials.

Graphite powder (*SDFCL* 99.5%), Sulphuric acid (H_2SO_4 *Molychem Ltd* 98 wt%,), Phosphoric acid (H_3PO_4, *s d Fine-Chem Ltd* 85%,), Potassium permanganate ($KMnO_4$, S*igma Aldrich* 99.4%), Hydrogen peroxide (H_2O_2, *s d Fine-Chem Ltd* 30%), Hydrochloric acid (HCl,

s d Fine-Chem Ltd 37%), Distilled water (DIW), Sodium hydroxide (NaOH, S*igma Aldrich* 97%), Blueberry and Silver nitrate ($AgNO_3$, S*igma Aldrich* 97%).

2.2. Preparation of GO.

Graphene oxide was synthesized via the Improved Hummers method [20] (Fig. 1). 120ml of sulphuric acid (H_2SO_4) and 13.33ml of phosphoric acid (H_3PO_4), i.e., in 9:1 ratio, was mixed and stirred for 25 minutes. Under the stirring condition, 1g of graphite powder was added. To the above solution, 5.867g of potassium permanganate ($KMnO_4$) was slowly added. This mixture was stirred for 6 hours until the solution became dark green. To eliminate the excess of $KMnO_4$, 3ml of hydrogen peroxide (H_2O_2) was added drop-wise and stirred for 10 minutes. An exothermic reaction occurs. Once the mixture was cooled down, it was continuously washed with hydrochloric acid (HCl) and deionized water (DIW) via centrifugation at 5000rpm for 15 minutes. The sample was then neutralized using sodium hydroxide (NaOH). Further, the sample was kept in a dialysis tube to remove unreacted ions. The sample was then dried in an oven at 70°C to obtain GO.

Figure 1. Schematic representation of the synthesis of graphene oxide.

2.3. Preparation of silver nanoparticles (AgNPs).

Silver nanoparticles were synthesized using a blueberry extract made from 100g of blueberry in 120 ml of DIW (Fig. 2). 0.1M of silver nitrate solution was prepared by adding 0.1698g of silver nitrate to 10ml of DIW. As prepared, 0.1M of silver nitrate solution was added drop-wise to 20ml of blueberry extract. The solution was kept overnight for stirring for the completion of the synthesis. The solution was then centrifuged for 20 minutes, and the collected residue was kept in the oven for drying at 90°C.

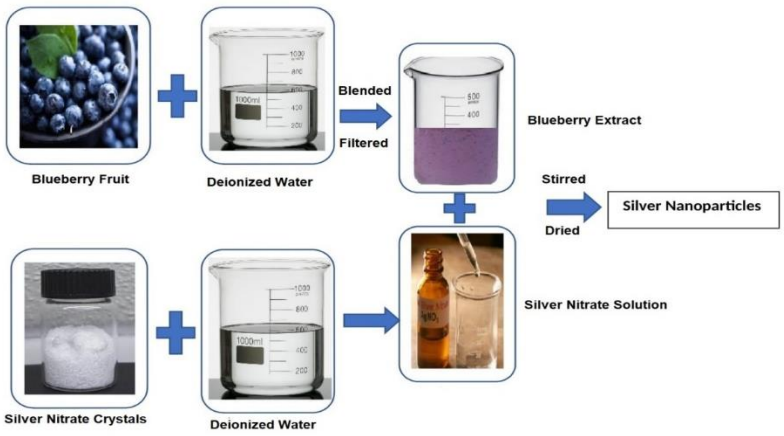

Figure 2. Schematic representation of the synthesis of silver nanoparticles.

2.4. Preparation of composites (GO-Ag).

The dried samples of GO and silver nanoparticles were physically mixed in a 90:10 ratio and then heated at 70°C.

2.5. Characterization techniques.

Crystallographic studies of samples were analyzed using an XRD diffractometer with Cu Kα as a radiation source. The structural parameters are calculated using the following relations:

$$\text{Interplanar spacing} = n\lambda / 2 \sin\theta \quad (1)$$

$$\text{Average crystallite size} = 1.84\lambda / \beta \cos\theta \quad (2)$$

$$\text{Lattice constant} = d\,(h^2 + k^2 + l^2)^{1/2} \quad (3)$$

$$\text{Microstrain} = \beta / 4 \tan\theta \quad (4)$$

FTIR absorption spectra of samples were obtained in the region of 500-4000 nm to analyze different functional groups in the sample. Optical properties and energy bandgap were determined using UV-Vis spectroscopy within the range of 200-800 nm. Raman spectroscopy was conducted for the wavelength ranging from 1000-1900 nm to measure the defect densities of the sample.

3. Results and Discussion

The XRD peaks reveal alterations in the chemical structure and crystalline configuration of the graphene matrix upon the incorporation of silver nanoparticles (Fig. 3). The XRD pattern of GO shows a characteristic peak at 2θ= 10.12° attributed to (001) plane [21]. It confirms the complete oxidation of graphite after acidic oxidation, and the interplanar spacing (d) is calculated to be 0.873 nm. An additional small diffraction peak is observed at 42.13º due to the (102) plane. The XRD pattern of AgNPs show four Bragg reflections at 38.28°, 44.46°, 64.66°, and 77.64° correspond to the planes of (111), (200), (220), and (311) respectively [22]. It substantiates the successful formation of face-centered cubic silver nanoparticles using the blueberry extract. The interplanar spacing for the (111) plane is found to be 0.235 nm.

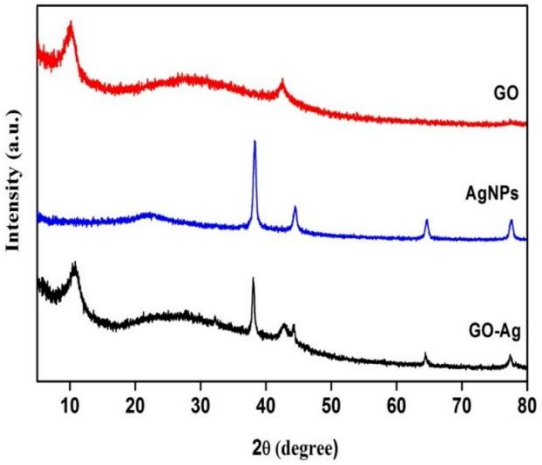

Figure 3. XRD pattern of GO, Ag nanoparticles, and GO-Ag composite.

The crystallite size, the lattice constant, cell volume, and microstrain of synthesized Ag nanoparticles were calculated and shown in Table 1. The observed defected peak of AgNPs anchored graphene sheets in the X-ray diffraction profile confirms the formation of GO-Ag nanocomposite. The peak at 2θ=10.12º is slightly shifted to 11.3º, indicating the reduction of GO upon deposition of Ag nanoparticles.

Table 1. Crystallite size, Lattice constant, Cell volume, and Microstrain of silver nanoparticles.

2θ	Crystallite size (nm)	Lattice constant (Å)	Cell volume(Å^3)	Microstrain
38.28^0	15.39	4.0689	67.3662	0.0068
44.46^0	12.52	4.0718	67.5131	0.0073
64.66^0	17.84	4.0737	67.6033	0.0036
77.64^0	17.55	4.0751	67.6767	0.0031

FTIR analysis was carried out to identify the functional groups localized on the surface of nanocomposites. As seen in Fig. 4, the prominent absorption band at ~3228cm^{-1} corresponds to the stretching vibrations of the C-OH (hydroxyl) group. FTIR spectra of GO show bands at 1724, 1652, 1336, and 1039.54cm^{-1} indicating the presence of C=O, C=C, C-O-C (epoxy), and C-O (alkoxy) stretching respectively [23,24]. The presence of numerous oxygen-containing functional groups over the graphene surface, confirm the successful synthesis of graphene oxide. The chemical moieties responsible for the reduction of silver salts into nanoparticles synthesized using blueberry extract are evident in the FTIR spectra of silver nanoparticles. The absorption band located between 3000-3500 cm^{-1} has an equal contribution from the O-H and N-H stretching. The sharp peak at 2927 cm^{-1} arises from C-H stretching of aromatic-compound like flavonoids contained in the fruit extract. Similarly, the bands at 1632 and 1380 cm^{-1} are assigned to the cyclobenzene and alkane groups, respectively. The C-O stretching of phytomolecules is observed at 1041 cm^{-1}. The small peak at 833 cm^{-1} corresponds to C=CH$_2$ [25-26]. Thus, FTIR analysis supports the presence of phenolic compounds and proteins, which facilitated the capping and stabilization of nanoparticles. The characteristic stretching of both GO and Ag nanoparticles observed in the IR spectra of nanohybrid substantiate the successful intercalation of silver nanoparticles within the Graphene matrix. For nanocomposite, the band (~3228cm^{-1}) due to the hydroxyl group has become broadened and less intense in comparison to bare GO. This is because the interaction between Ag^+ and oxygen-containing functional group results in the reduction of GO [27].

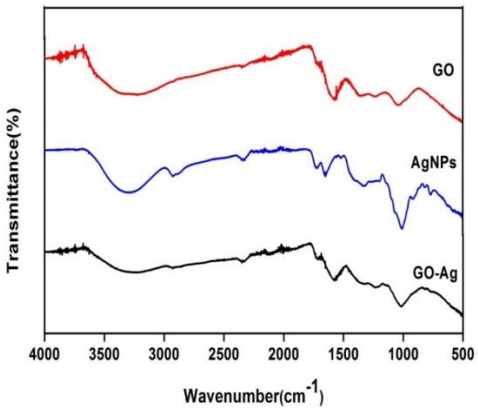

Figure 4. FTIR spectra of GO, Ag nanoparticle, and GO-Ag composites.

Raman spectroscopy was employed to comprehend the graphitization degree and carbon bond structures in the synthesized samples. The most prominent features in Raman spectra of graphitic materials are the D and G bands that arise from the vibrations of sp^2 hybrid

carbon atoms and disordered structures, respectively [28]. As seen in Fig. 5, the D band of GO occurs at 1323 cm^{-1} while G band at 1584 cm^{-1}. The Raman spectra of nanocomposite exhibited peaks similar to that of bare GO but are of higher intensities. Furthermore, the GO-Ag nanocomposite displayed peaks due to the graphitic band (G-band) at 1334 cm^{-1} and defect band (D-band) at 1597 cm^{-1}. The redshift in the peak position can be explained in terms of the charge transfer between silver nanoparticles and GO surface [29]. The relative intensity ratio of D band to G-band (I_D/I_G) measures the degree of defects in the graphene domain. The I_D/I_G ratio of GO and GO-Ag is calculated to be 0.99 and 1.06, respectively.

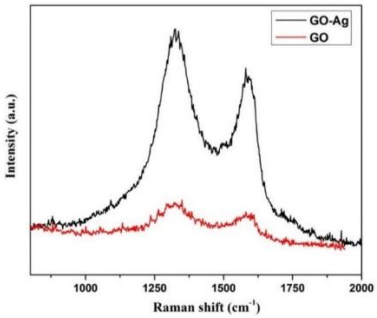

Figure 5. Raman spectra of GO and GO-Ag composite.

The absorption and the conjugated network of synthesized samples were elucidated using UV-Vis spectroscopy. From Fig.6a, it can be inferred that GO possesses a dominant absorption band at 250 nm owing to the π-π^*transition of the plasmon peak. This peak arises due to the contribution from sp^2 clusters as well as chromophore units such as C=C. A small shoulder peak observed near 300 nm is attributed to n-π^*transition of C=O [30,31]. The UV-Vis spectrum of silver nanoparticles shows a characteristic surface plasmon peak around 430 nm. The free electrons of the metal undergo mutual interaction in resonance with the incident light wave and hence yield the surface plasmon resonance (SPR) absorption band [32]. In the case of GO-Ag nanocomposite, the broad peak observed around 350-450 nm caused by the SPR confirms the deposition of Ag nanoparticles over the graphene surface. However, the peak at 250 nm of GO dispersion was redshifted to 275 nm suggesting the reduction of graphene oxide [33].

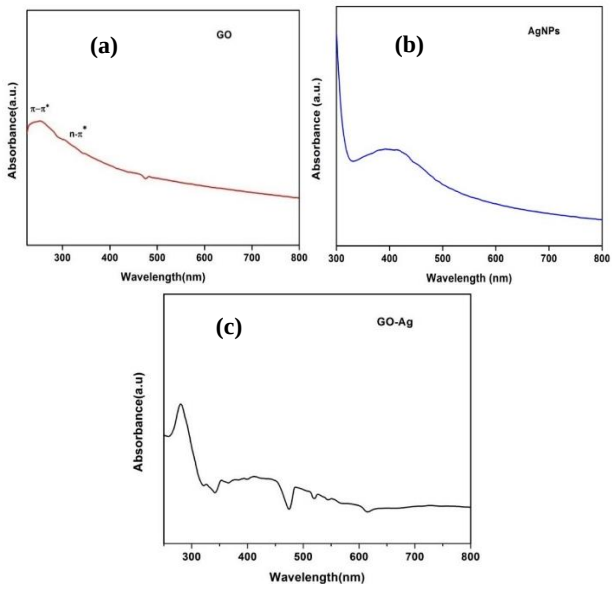

Figure 6. UV-Vis spectra of (**a**) GO; (**b**) Ag nanoparticle; (**c**) GO-Ag composites.

The optical bandgap of GO was determined using the Tauc plot with a linear extrapolation towards the energy axis. The amorphous GO sheet having a non-uniform oxidation level cannot exhibit sharp absorption edges in the Tauc plot [34]. The bandgap of GO and silver nanoparticles from Fig.7 is estimated to be 3.41and 2.28 eV, respectively. The bandgap value of composite (2.33 eV) is found to be smaller than GO. The decrease in the bandgap is due to the introduction of dopant, which is more conductive compared to GO [35]. Hence it is found that the decoration of Ag nanoparticles over the GO surface helps in controlled reduction favorable for tuning of bandgap and dynamic optical properties.

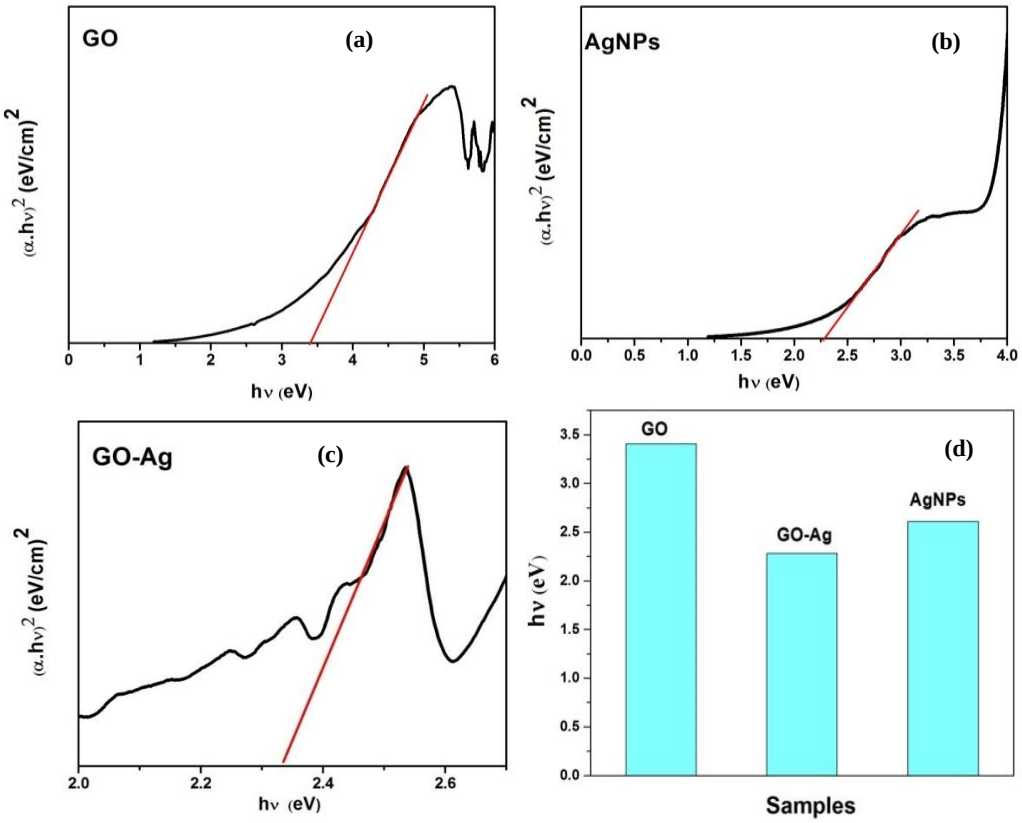

Figure 7. Tauc plots of (**a**) GO; (**b**) Ag nanoparticle; (**c**) GO-Ag composites; (**d**) Bar diagram depicting variation in the bandgap.

4. Conclusions

In the present study, GO-Ag nanocomposite was successfully fabricated via an eco-friendly synthesis route. Graphene oxide was prepared using improved Hummer's method without using toxic $NaNO_3$. A plant-mediated synthesis was employed for the synthesis of silver nanoparticles. The fruit extract of *cyanococcus* was used as the reducing and stabilizing agent for the preparation of silver nanoparticles. These biosynthesized nanoparticles were impregnated into the graphene matrix for the formation of GO-Ag nanocomposite. The XRD and FTIR analysis confirmed the successful deposition of AgNPs over the GO surface. The reduction of GO observed in the nanocomposite suggest the interaction between Ag^+ and oxygen functional group. The redshift of the Raman peaks gives evidence of the charge transfer process among GO and silver nanoparticles. UV-Vis spectroscopy gave an idea about the variation in energy bandgap with the addition of AgNPs. The results clearly show the transition of optical bandgap from insulating to the semiconducting range. This proposed method is a green initiative for developing semiconducting nanocomposite, having extended practicalities.

Funding

This research received no external funding.

Acknowledgments

We are grateful to the Department Of Physics and Electronics, CHRIST (Deemed to be University), in support of project funding and lab facilities.

Conflicts of Interest

The authors declare no conflict of interest.

References

1. Naghibi, S.; Kargar, F.; Wright, D.; Huang, C.Y.T.; Mohammadzadeh, A.; Barani, Z.; Salgado, R.; Balandin, A.A. Noncuring Graphene Thermal Interface Materials for Advanced Electronics. *Advanced Electronic Materials* **2020**, *6*, https://doi.org/10.1002/aelm.201901303.
2. Kashte, S.; Sharma, R.K.; Kadam, S. Layer-by-layer deposited osteoinductive scaffolds for bone tissue engineering. *Letters in Applied Nanobioscience*. **2020,** *9*, 1089-1098, https://doi.org/10.33263/LIANBS92.10891098.
3. Wang, R.; Xu, Z.; Zhuang, J.; Liu, Z.; Peng, L.; Li, Z.; Liu, Y.; Gao, W.; Gao, C. Highly Stretchable Graphene Fibers with Ultrafast Electrothermal Response for Low-Voltage Wearable Heaters. *Advanced Electronic Materials* **2017**, *3*, 1600425, https://doi.org/10.1002/aelm.201600425.
4. Omar, S.; van Wees, B.J. Spin transport in high-mobility graphene on WS2 substrate with electric-field tunable proximity spin-orbit interaction. *Physical Review B* **2018**, *97*, 045414, https://doi.org/10.1103/PhysRevB.97.045414.
5. Elazab, H.A.; Gadall, M.; Sadek, M.A.; El-Idreesy, T.T. Hydrothermal Synthesis of Graphene supported Pd/Fe3O4 Nanoparticles as an Efficient Magnetic Catalysts for Suzuki Cross–Coupling. *Biointerface Research in Applied Chemistry* **2019**, *9*, 2. https://doi.org/10.33263/BRIAC92.906911.
6. Manoj, B.; Kunjomana, A.G. Systematic investigations of graphene layers in sub-bituminous coal. *Russ. J. Appl. Chem.* **2014**, *87*, 1726-1733, https://doi.org/10.1134/S1070427214110251.
7. Krishnan, R.; Balachandran, M. Transformation of hydrocarbon soot to graphenic carbon nanostructures. *Biointerface Research In Applied Chemistry* **2018**, *8*, 3187-3192.
8. Jing, B.; Ao, Z.; Teng, Z.; Wang, C.; Yi, J.; An, T. Density functional theory study on the effects of oxygen groups on band gap tuning of graphitic carbon nitrides for possible photocatalytic applications. *Sustainable Materials and Technologies* **2018**, *16*, 12-22, https://doi.org/10.1016/j.susmat.2018.04.001.
9. Jin, Y.; Zheng, Y.; Podkolzin, S.G.; Lee, W. Band gap of reduced graphene oxide tuned by controlling functional groups. *Journal of Materials Chemistry C* **2020**, *8*, 4885-4894, https://doi.org/10.1039/C9TC07063J.
10. Manoj, B.; Raj, A.M.; Thomas, G.C. Tailoring of low grade coal to fluorescent nanocarbon structures and their potential as a glucose sensor. *Sci. Rep.* **2018**, *8*, 13891, https://doi.org/10.1038/s41598-018-32371-9.
11. Nair, A.V.; Manoj, B. Tailoring of Energy Band Gap inGraphene-like System by Fluorination. *Mapana Journal of Sciences* **2019**, *18*, 55-66, https://doi.org/10.12723/mjs.48.4.
12. Mohan, A.N.; B, M. Extraction of Graphene Nanostructures from Colocasia esculenta and Nelumbo nucifera Leaves and Surface Functionalization with Tin Oxide: Evaluation of Their Antibacterial Properties. *Chemistry – A European Journal* **2020**, *26*, 8105-8114, https://doi.org/10.1002/chem.202000590.
13. Hamzah, M.; Khenfouch, M.; Srinivasu, V.V. The quenching of silver nanoparticles photoluminescence by graphene oxide: spectroscopic and morphological investigations. *Journal of Materials Science: Materials in Electronics* **2017**, *28*, 1804-1811, https://doi.org/10.1007/s10854-016-5729-1.
14. Williams, G.; Kamat, P.V. Graphene−Semiconductor Nanocomposites: Excited-State Interactions between ZnO Nanoparticles and Graphene Oxide. *Langmuir* **2009**, *25*, 13869-13873, https://doi.org/10.1021/la900905h.
15. Chazalviel, J.-N.; Allongue, P. On the Origin of the Efficient Nanoparticle Mediated Electron Transfer across a Self-Assembled Monolayer. *J. Am. Chem. Soc.* **2011**, *133*, 762-764, https://doi.org/10.1021/ja109295x.
16. Das, M.R.; Sarma, R.K.; Borah, S.C.; Kumari, R.; Saikia, R.; Deshmukh, A.B.; Shelke, M.V.; Sengupta, P.; Szunerits, S.; Boukherroub, R. The synthesis of citrate-modified silver nanoparticles in an aqueous suspension of graphene oxide nanosheets and their antibacterial activity. *Colloids Surf. B. Biointerfaces* **2013**, *105*, 128-136, https://doi.org/10.1016/j.colsurfb.2012.12.033.
17. Manoj, B.; Ashlin, M.R.; George Thomas, C. Facile synthesis of preformed mixed nano-carbon structure from low rank coal. *Materials Science-Poland* **2018**, *36*, 14-20, https://doi.org/10.1515/msp-2018-0026.

18. Wadhwa, H.; Kumar, D.; Mahendia, S.; Kumar, S. Microwave assisted facile synthesis of reduced graphene oxide-silver (RGO-Ag) nanocomposite and their application as active SERS substrate. *Mater. Chem. Phys.* **2017**, *194*, 274-282, https://doi.org/10.1016/j.matchemphys.2017.03.045.
19. Kumari, S.; Sharma, P.; Yadav, S.; Kumar, J.; Vij, A.; Rawat, P.; Kumar, S.; Sinha, C.; Bhattacharya, J.; Srivastava, C.M.; Majumder, S. A Novel Synthesis of the Graphene Oxide-Silver (GO-Ag) Nanocomposite for Unique Physiochemical Applications. *ACS Omega* **2020**, *5*, 5041-5047, https://doi.org/10.1021/acsomega.9b03976.
20. Manoj, B. Synthesis and characterization of porous, mixed phase, wrinkled, few layer graphene like nanocarbon from charcoal. *Russian Journal of Physical Chemistry A* **2015**, *89*, 2438-2442, https://doi.org/10.1134/S0036024415130257.
21. Mututu, V.; Thomas, R.; Pandey, M.; Balachandran, M. An Investigation on Structural, Electrical and Optical properties of GO/ZnO Nanocomposite. *International journal of electrochemical science* **2019**, 3752-3763, https://doi.org/10.20964/2019.04.49.
22. Mohan, A.N.; B, M. Biowaste derived graphene quantum dots interlaced with SnO2 nanoparticles – a dynamic disinfection agent against Pseudomonas aeruginosa. *New J. Chem.* **2019**, *43*, 13681-13689, https://doi.org/10.1039/C9NJ00379G.
23. Mohan, A.N.; Manoj, B. Surface modified graphene/SnO2 nanocomposite from carbon black as an efficient disinfectant against Pseudomonas aeruginosa. *Mater. Chem. Phys.* **2019**, *232*, 137-144, https://doi.org/10.1016/j.matchemphys.2019.04.074.
24. Thomas, R.; Jayaseeli, E.; Sharma, N.M.S.; Manoj, B. Opto-electric property relationship in phosphorus embedded nanocarbon. *Results in Physics* **2018**, *10*, 633-639, https://doi.org/10.1016/j.rinp.2018.07.018.
25. Li, K.; Ma, C.; Jian, T.; Sun, H.; Wang, L.; Xu, H.; Li, W.; Su, H.; Cheng, X. Making good use of the byproducts of cultivation: green synthesis and antibacterial effects of silver nanoparticles using the leaf extract of blueberry. *J. Food Sci. Technol.* **2017**, *54*, 3569-3576, https://doi.org/10.1007/s13197-017-2815-1.
26. Pathak, J.; Sonker, A.S.; Singh, R.V.; Kumar, D.; Sinha, R.P. Synthesis of silver nanoparticles from extracts of Scytonema geitleri HKAR-12 and their in vitro antibacterial and antitumor potentials. *Letters in Applied NanoBioScience*. **2019**, *8*, 576-85. https://doi.org/10.33263/LIANBS83.576585
27. Vi, T.T.T.; Rajesh Kumar, S.; Rout, B.; Liu, C.-H.; Wong, C.-B.; Chang, C.-W.; Chen, C.-H.; Chen, D.W.; Lue, S.J. The Preparation of Graphene Oxide-Silver Nanocomposites: The Effect of Silver Loads on Gram-Positive and Gram-Negative Antibacterial Activities. *Nanomaterials* **2018**, *8*, 163, https://doi.org/10.3390/nano8030163.
28. Huang, H.; Li, Z.; She, J.; Wang, W. Oxygen density dependent band gap of reduced graphene oxide. *J. Appl. Phys.* **2012**, *111*, 054317, https://doi.org/10.1063/1.3694665.
29. Mariappan, S.M.; Karthikeyan, B. Optical and Vibrational Properties of Ag Nanometal-Enhanced Blue Light-Emitting Graphene Oxide-Polyvinylpyrrolidone Polymer Composite Films. *Plasmonics* **2017**, *12*, 171-177, https://doi.org/10.1007/s11468-016-0245-y.
30. de Lima, A.H.; Tavares, C.T.; da Cunha, C.C.S.; Vicentini, N.C.; Carvalho, G.R.; Fragneaud, B.; Maciel, I.O.; Legnani, C.; Quirino, W.G.; de Oliveira, L.F.C.; Sato, F.; de Mendonça, J.P.A. Origin of optical bandgap fluctuations in graphene oxide★. *Eur. Phys. J. B* **2020**, *93*, https://doi.org/10.1140/epjb/e2020-100578-7.
31. B, M.; Raj, A.M.; Chirayil, G.T. Tunable direct band gap photoluminescent organic semiconducting nanoparticles from lignite. *Sci. Rep.* **2017**, *7*, 18012, https://doi.org/10.1038/s41598-017-18338-2.
32. Njagi, E.C.; Huang, H.; Stafford, L.; Genuino, H.; Galindo, H.M.; Collins, J.B.; Hoag, G.E.; Suib, S.L. Biosynthesis of Iron and Silver Nanoparticles at Room Temperature Using Aqueous Sorghum Bran Extracts. *Langmuir* **2011**, *27*, 264-271, https://doi.org/10.1021/la103190n.
33. Liu, G.-f.; Huang, L.-j.; Wang, Y.-x.; Tang, J.-g.; Wang, Y.; Cheng, M.-m.; Zhang, Y.; Kipper, M.J.; Belfiore, L.A.; Ranil, W.S.Preparation of a graphene/silver hybrid membrane as a new nanofiltration membrane. *RSC Advances* **2017**, *7*, 49159-49165, https://doi.org/10.1039/c7ra07904d.
34. Salimeh, K.; Fahimeh, A. Effect of temperature on the structural, linear, and nonlinear optical properties of MgO-doped graphene oxide nanocomposites. *Nanophotonics* **2018**, *7*, 243-251, https://doi.org/10.1515/nanoph-2017-0030.
35. Maharubin, S.; Zhang, X.; Zhu, F.; Zhang, H.-C.; Zhang, G.; Zhang, Y. Synthesis and Applications of Semiconducting Graphene. *Journal of Nanomaterials* **2016**, *2016*, 6375962, https://doi.org/10.1155/2016/6375962.